

Document downloaded from:

<http://hdl.handle.net/10251/98352>

This paper must be cited as:

Santacatalina Bonet, JV.; Guerrero, M.; García Pérez, JV.; Mulet Pons, A.; Carcel Carrión, JA. (2016). Ultrasonically assisted low-temperature drying of desalted codfish. Food Science and Technology Research. 65:444-450. doi:10.1016/j.lwt.2015.08.023



The final publication is available at

<https://doi.org/10.1016/j.lwt.2015.08.023>

Copyright Japanese Society for Food Science and Technology

Additional Information

1 **ULTRASONICALLY ASSISTED LOW-TEMPERATURE DRYING OF DESALTED**
2 **CODFISH**

3 J.V. Santacatalina, M.E. Guerrero, J.V. Garcia-Perez, A. Mulet and J.A. Cárcel*

4

5 Grupo ASPA, Departamento de Tecnología de Alimentos, Universitat Politècnica de
6 València, Camí de Vera s/n, E46022, València, Spain.

7

8

9

10

11

12

13

14

15

16 *Corresponding author. Tel.: +34 96 3879365; Fax: +34 96 3879839. E-mail address:

17 jcarcel@tal.upv.es (J.A. Cárcel).

18

19 **Abstract**

20 Low-temperature drying (LTD) constitutes an interesting means of dehydrating
21 foodstuffs, thus preserving the quality of the product. Power ultrasound (US) generates
22 several mechanical effects that could help to shorten the long drying times associated
23 with LTD. In this work, the feasibility of using US in LTD of desalted cod was assessed.

24 For this purpose, desalted cod slices (50x30x5 mm) were dried (2 m/s) at different
25 temperatures (10, 0 and -10°C) without (AIR) and with (AIR+US, 20.5 kW/m³) US
26 application. Afterwards, the dried samples were rehydrated in distilled water (25°C). A
27 diffusion model was used to describe both drying and rehydration kinetics. The color
28 and hardness of both dried and rehydrated cod samples were also measured.

29 The application of US increased the drying rate at every temperature tested,
30 shortening the drying time by 16% at 0°C and up to 60% at -10°C. The ultrasonically
31 assisted dried samples presented a rehydration rate which was slightly lower than that
32 of those that had been conventionally dried, but they were harder and whiter, which is
33 more suited to consumer preferences. Therefore, power ultrasound could be
34 considered an affordable technology with which to accelerate LTD of desalted cod,
35 providing high quality dried products.

36

37 **Keywords:** Ultrasound; Dehydration; Rehydration; Texture; Color

38

39 1. Introduction

40 Dried and salt-cured cod (*Gadus morhua*) is a highly-appreciated product due to its
41 high nutritional value (high protein and low fat content) and its particular sensory
42 properties. It is mainly produced in Norway and Iceland and primarily consumed in the
43 Southern European countries, such as Spain and Portugal (Martínez-Álvarez and
44 Gómez-Guillén, 2013; Oliveira, Pedro, Nunes, Costa, and Vaz-Pires, 2012). The high
45 salt concentration of this product (approximately 20% w/w) prevents its degradation but
46 limits its direct consumption; for this reason salted cod must be desalted (Ozuna, Puig,
47 Garcia-Perez, and Cárcel, 2014a), a process that takes approximately 24h. This slow
48 salt diffusion constrains the consumption of salted cod for both domestic use and the
49 catering industry. In addition, the desalting converts the cod into a highly perishable
50 product (Fernández-Segovia, Escriche, Fuentes, and Serra, 2007) and, in fact, the fish
51 must be either immediately consumed, chilled or frozen (Lauritzsen et al., 2004).
52 Therefore, it could be interesting to explore alternative preservation methods, such as
53 drying, that ensure both the desalted product's stability and the retention of the sensory
54 attributes (Andrés, Rodríguez-Barona, and Barat, 2005). The desalted and dried cod
55 may be used as an ingredient in prepared foods, such as instant meals or ready-to-use
56 products, due to its low salt content and rehydration ability.

57 Convective drying constitutes a traditional dehydration method for foodstuffs (Garcia-
58 Perez, Ozuna, Ortuño, Cárcel, and Mulet, 2011). The use of high air temperatures
59 accelerates the drying kinetics, but causes chemical and physical changes that can
60 affect the quality traits of the dried product (Soria et al., 2010). Consumer demand for
61 high quality products has encouraged research into alternative techniques to minimize
62 quality degradation during processing. In this sense, low temperature drying (LTD)
63 could be an interesting method. However, the long drying times linked to LTD could
64 limit its use on an industrial scale.

65 Power ultrasound (US) has been used to speed up the convective drying of several
66 foodstuffs (Cárcel, Garcia-Perez, Riera, and Mulet, 2011; Gallego-Juárez et al., 2007;
67 Garcia-Perez et al., 2011), mainly by introducing mechanical energy. The ultrasonic
68 waves generate alternating expansions and contractions when travelling across a
69 medium, which have a similar effect to that found in a sponge when it is repeatedly
70 squeezed and released (Gallego Juárez et al., 2007). This mechanical stress helps the
71 water move from the inner parts of the product to the surface and could create
72 microscopic channels that reduce the internal resistance to mass transfer (Gallego-
73 Juárez, 2010). Moreover, in solid/gas systems, the application of US also produces
74 oscillating velocities, micro-streaming and pressure variation at the interfaces, which
75 reduce the boundary layer and, as a consequence, improve water movement from the
76 solid surface to air. Therefore, US could help to reduce both the external and the
77 internal mass transfer resistance without introducing a significant amount of thermal
78 energy during drying (Cárcel et al., 2011). In this sense, the feasibility of US application
79 during the LTD process of different products, such as apple (Santacatalina et al., 2014,
80 Garcia-Perez, Cárcel, Riera, Rosselló, and Mulet, 2012), salted cod (Ozuna, Cárcel,
81 Walde, and Garcia-Perez, 2014b), green peas (Bantle and Eikevik, 2011), carrot or
82 eggplant (Garcia-Pérez et al., 2012) has been proved. More research has been done
83 on analyzing the effect of US on the drying kinetics than on the product quality (Pingret,
84 Fabiano-Tixier, and Chemat, 2013). Therefore, the aim of this work was to evaluate the
85 feasibility of using US in LTD of desalted cod, analyzing not only drying and rehydration
86 kinetics but also quality parameters, such as color and texture.

87

88 **2. Materials and methods**

89 *2.1. Raw material and sample preparation*

90 A homogeneous batch of salted cod (*Gadus morhua*) was provided by a local supplier
91 (Carmen Cambra S. L., Spain). The pieces of salted cod averaged 1.5 ± 0.25 kg.

92 Parallelepiped-shaped samples (50x30x5 mm) were obtained from the central part of
93 the cod loin using a sharp knife and, afterwards, were wrapped in plastic waterproof
94 film and kept refrigerated at $2\pm 1^{\circ}\text{C}$ (maximum storage time 120 h) until the desalting
95 process took place. For that purpose, the slices of salted cod were immersed in water
96 (70 g cod/L water) of low mineral content (Cortes S.A., Spain) at $4\pm 1^{\circ}\text{C}$ for 24 h. After
97 desalting, the surface water was removed with tissue paper. Then the samples were
98 wrapped in plastic waterproof film and separated into three batches. Two of them were
99 kept in refrigeration at $2\pm 1^{\circ}\text{C}$ (maximum storage time 4 h) until the drying experiments
100 were conducted (samples dried at 0 and 10°C). The third (samples dried at -10°C) was
101 frozen by placing samples at $-18\pm 1^{\circ}\text{C}$ until processing (at least 72 h).

102 The moisture and the NaCl content of the cod samples were measured before and
103 after desalting following standard methods 950.46 and 971.27, respectively (AOAC,
104 1997). Thus, the moisture content was obtained by the difference of weighting
105 between salted or desalted cod samples and the same cod samples dried at 105°C
106 until they achieved constant weight (24 h approximately). For the NaCl measurement,
107 approximately 0.5 g of ground sample was placed into 100 mL of distilled water and
108 homogenised at 9500 r.p.m. for 5 min with an ultra-turrax mod. T25 provided with a
109 dispersion tool mod. S25N-18G (IKA Labortechnik, Janke & Kunkel GMBH & Co,
110 Staufen, Germany). The chloride content of the extract was determined in triplicate
111 using a chloride meter (Ciba Corning, mod. 926. L; Halstead, Essex, United Kingdom).
112 Thus, the average value of the moisture content of desalted cod was 4.42 ± 0.02 kg
113 water/kg dry matter of desalted cod (dmdc) and the NaCl content was 0.023 ± 0.001 kg
114 NaCl/kg dmdc.

115

116 *2.2. Drying experiments*

117 Drying experiments were carried out in a convective drier with air recirculation (Figure
118 1), already described in the literature (Garcia-Perez et al., 2012). The system provides
119 an automatic temperature and air velocity control. Moreover, an ultrasonically activated
120 cylindrical radiator generates a high intensity ultrasonic field (155 dB) in the drying
121 chamber. Drying experiments were conducted using a constant air velocity (2 m/s) at
122 three different temperatures (10, 0 and -10°C), without (AIR) and with (AIR+US, 20.5
123 kW/m³) US application. Drying kinetics were obtained by weighing samples at preset
124 times (interval of 15 min) and considering the initial moisture content. In every case, the
125 initial mass load was of 138.7±6.9 g (10 cod slices) and the relative humidity of drying
126 air was maintained below 10±3% during the whole drying process.

127 The drying experiments were replicated at least three times for each drying condition
128 tested and extended until samples lost 65±3% of the initial weight. After drying, the
129 moisture content of the samples was also measured following standard method 950.46
130 (AOAC, 1997). Finally, the dried samples were vacuum-sealed and stored in
131 refrigeration (0±1°C; maximum storage time 4 days) until the quality analyses
132 (rehydration, color and texture) were carried out.

133

134 *2.3. Modeling of drying kinetics*

135 A diffusion model was used to describe the drying kinetics. The mass transport was
136 considered to be one-dimensional due to the fact that sample thickness (5 mm) was
137 1/6 (30 mm) and 1/10 (50 mm) shorter than the other dimensions. Thus, the approach
138 of considering the samples as infinite slabs can be considered as appropriate (Garau,
139 Simal, Femenia, and Rosselló, 2006). Assuming the effective moisture diffusivity as
140 constant and the solid to be isotropic and homogeneous, the diffusion equation
141 (equation 1) is written as follows:

142
$$\frac{\partial W_p(x,t)}{\partial t} = D_{ed} \left(\frac{\partial^2 W_p(x,t)}{\partial x^2} \right) \quad (1)$$

143 where W_p is the local moisture (kg water/kg dmdc), t is the time (s), D_{ed} is the effective
 144 moisture diffusivity (m^2/s) during drying and x represents the characteristic mass
 145 transport direction in the slab geometry (m).

146 In order to solve equation (1), the following assumptions were considered: solid
 147 symmetry, uniform initial moisture content and temperature, constant shape during
 148 drying and negligible external resistance to mass transfer. The analytical solution of the
 149 diffusion equation, expressed in terms of the average moisture content, is shown in
 150 equation (2) (Crank, 1975).

151
$$W(t) = W_e + (W_0 - W_e) \left[2 \sum_{n=0}^{\infty} \frac{1}{\lambda_n^2 L^2} e^{-D_{ed} \lambda_n^2 t} \right] \quad (2)$$

152 where, λ_n are the eigenvalues calculated as $\lambda_n L = (2n + 1) \frac{\pi}{2}$, W is the average
 153 moisture content (kg water/kg dmdc), L the half-thickness of the sample (m) and
 154 subscripts 0 and e represent the initial and equilibrium state, respectively.

155 The diffusion model was fitted to the experimental drying kinetics in order to identify the
 156 effective moisture diffusivity. The identification was carried out by minimizing the sum
 157 of the squared differences between the experimental and the calculated average
 158 moisture content. For that purpose, the Generalized Reduced Gradient (GRG)
 159 optimization method, available in Microsoft Excel™ spreadsheet (Microsoft
 160 Corporation, Seattle, WA, USA) was used. The goodness of the fit was determined by
 161 calculating the percentage of explained variance (VAR, equation 3).

162
$$VAR = \left[1 - \frac{S_{xy}^2}{S_y^2} \right] \cdot 100 \quad (3)$$

163 where S_{xy} and S_y are the standard deviation of the estimation and the sample,
 164 respectively.

165

166 2.4. Rehydration experiments

167 The rehydration capacity was determined by immersing the dried cod samples in
168 distilled water at $25\pm 1^\circ\text{C}$. In order to obtain the rehydration kinetics, the samples were
169 taken out of the bath at preset times, blotted with tissue paper to remove the surface
170 water and weighed. The rehydration tests were carried out in triplicate for each drying
171 condition considered, using 10 samples (16.5 ± 1.5 g) of dried cod in each run. The
172 experiments were extended until the difference in sample weight between two
173 consecutive measurements (60 min) was lower than 0.5 g, assuming that this point
174 was close to the equilibrium weight. The rehydration kinetics were modeled using the
175 same diffusion model described in section 2.3. for the drying kinetics. In this case, W_0
176 represents the moisture content of the dried samples and W_e the equilibrium moisture
177 content of the rehydrated samples and the term D_{ed} was replaced by D_{er} to differentiate
178 the effective moisture diffusivity (m^2/s) during drying and rehydration.

179

180 2.5. Color

181 The color of both dried and rehydrated cod samples was determined by measuring the
182 CIE $L^*a^*b^*$ color coordinates (Bai, Sun, Xiao, Mujumdar, and Gao, 2013) using a
183 colorimeter (Minolta CM-2500d, Konica Minolta Optics, Inc., Japan), provided with a
184 standard illuminant D65, an observation angle of 10° and calibrated using a standard
185 white. In every case, the measurements were carried out directly on the sample
186 surface, in triplicate and at room temperature ($20\pm 1^\circ\text{C}$). Thus, for each type of dried
187 sample, a minimum of 90 color measurements were carried out. The overall color
188 difference (ΔE , equation 4) was computed as the difference between AIR+US (L^* , a^* ,
189 b^*) and AIR (L_0^* , a_0^* , b_0^*) samples. In the case of the rehydrated samples, ΔE indicates

190 the color difference between the rehydrated samples (L^* , a^* , b^*) and the desalted cod
191 before drying (L_0^* , a_0^* , b_0^*).

$$192 \quad \Delta E = \sqrt{(L^* - L_0^*)^2 + (a^* - a_0^*)^2 + (b^* - b_0^*)^2} \quad (4)$$

193

194 2.6. Texture

195 The hardness of both dried and rehydrated cod samples was measured using a
196 Texture Analyzer (TAX-T2, Stable Micro System, Godalming, United Kingdom) with a
197 load cell of 25 kg. The penetration tests were conducted with a 2 mm flat cylinder probe
198 (SMS P/2N), at a crosshead speed of 1 mm/s and a strain of 75% (penetration distance
199 3.5 mm). The hardness was characterized as the maximum penetration force achieved.
200 In each sample, the penetration tests were carried out at 16 points following a preset
201 pattern. For each drying run, at least three dried and three rehydrated samples were
202 analyzed. Because each drying conditions was tested by triplicate, this means that nine
203 dried and nine rehydrated samples was used to assess the hardness in each case.

204

205 2.7. Statistical analysis

206 Analyses of variance (ANOVA) ($p < 0.05$) were carried out and LSD (Least Significant
207 Difference) intervals were estimated using the statistical package, Statgraphics
208 Centurion XVI (Statpoint Technologies Inc., Warrenton, VA, USA), in order to assess
209 the significance of the influence of the different operating conditions (temperature and
210 US application) on the identified D_{ed} and D_{er} , as well as on the color and hardness of
211 both the dried and rehydrated samples.

212

213 3. Results and discussion

214 3.1. Drying experiments

215 The drying kinetics of desalted cod without (AIR) and with (AIR+US) ultrasound
216 application are shown in Figure 2. In both AIR and AIR+US, the lower the drying
217 temperature, the longer the drying time. Thus, in AIR experiments, 69% less time was
218 needed for drying at 10°C (18.1±1.9 h) than at -10°C (57.7±5.9 h). It should be noted
219 that at 0 and 10°C, the water was removed from the solid matrix by evaporation. On the
220 contrary, at -10°C, water removal took place by sublimation due to the fact that the
221 water remains frozen during drying; therefore, under these conditions it could be
222 considered as atmospheric freeze drying (AFD) (Claussen, Ustad, Strommen, and
223 Walde, 2007).

224 The application of US increased the drying rate at every temperature tested (Figure 2).
225 The shortening of the drying time depended on the temperature being higher at -10°C
226 (60%) than at 0 and 10°C (16 and 29%, respectively). As observed in Figure 2, the
227 influence of temperature on AIR+US drying kinetics was less remarkable than in AIR
228 experiments. Thus, the difference in drying time between the AIR experiments carried
229 out at -10 and 10°C was 39.6 h, while this difference was only 10.2 h in the case of
230 AIR+US experiments. Using the same US device, Ozuna et al. (2014b) succeeded in
231 shortening the drying time by between 35 and 54% when US was applied during the
232 drying of salted cod (from -10 to 20°C). In the case of apple drying, and under similar
233 experimental conditions (from -10 to 10°C), Santacatalina et al. (2014) found time
234 savings of between 60 and 77%. Likewise, Garcia-Perez et al. (2012) reported drying
235 time reductions of around 70% in the drying of carrot and eggplant at -14°C. Bantle and
236 Hanssler (2013) reduced the drying time by over 90% when drying salted codfish at
237 10°C using a commercial ultrasonic plate-like emitter (20kHz; DN 20/200, Sonotronic,
238 Karnsbald, Germany), but considering only the initial drying period (until samples
239 reached a moisture content of 45%). Schössler, Jäger, and Knorr (2012) reported that,
240 when freeze-drying red bell pepper cubes using a contact ultrasonic system, the drying
241 time was shortened by 11.5%.

242

243 *3.2. Modeling of drying kinetics*

244 The proposed model was adequate for describing the drying kinetics of desalted cod
245 slices at 0 and 10°C, obtaining percentages of explained variance (VAR) of over 99%
246 (Table 1). The goodness of the fit at 0 and 10°C is illustrated in Figure 2, where the
247 similar trend of the experimental and calculated moisture content can be observed. On
248 the contrary, a lower VAR value (98.5%) was found in the experiments carried out at -
249 10°C, probably because the samples remain frozen during drying. Under these
250 conditions, the water is removed by sublimation and two layers can be found in the
251 product: a frozen inner core and a dry outer layer. Therefore, the product is not
252 homogeneous, as is assumed in the diffusion model.

253 At the drying temperatures tested, the fit of the diffusion model was poorer when US
254 was applied. This is probably due to the fact that US application partially modifies the
255 mechanisms of mass transport that could affect the relationship between internal and
256 external mass transport resistance, meaning that diffusion was not the only mechanism
257 controlling mass transfer, as assumed in the model.

258 In any case, in the proposed model, any effect on the drying rate was included in the
259 D_{ed} . Therefore, this parameter can be used to compare and assess the overall effect of
260 the different conditions tested (temperature and/or US application) on the drying rate.

261 In the case of temperature, the higher the air drying temperature applied, the higher the
262 identified D_{ed} (Table 1). The application of US during LTD of desalted cod also involved
263 a significant ($p < 0.05$) increase in the D_{ed} at the three temperatures studied (Table 1).

264 This influence of US on the identified diffusivities were similar to those reported by
265 Ozuna et al. (2014b) for US-assisted drying kinetics of salted cod at temperatures
266 between 20 and -10°C. The mechanical stress caused by the alternating compressions
267 and expansions (sponge effect) produced by US could improve the internal diffusion of
268 moisture (Gallego-Juárez et al., 2007). Moreover, this stress could create microscopic

269 channels that help to make the movement of the water towards the product surface
270 easier (Gallego-Juárez, 2010). At the solid-air interface, US produces alternating
271 pressures and microstirring that could also help to speed-up the convective moisture
272 transport.

273 As can be observed in Table 1, the increase in D_{ed} produced by US application was
274 significantly ($p<0.05$) larger in the experiments conducted at -10°C (123.5%) than in
275 those carried out at 0 and 10°C (17.4 and 35.4%, respectively). As stated before, while
276 evaporation was responsible for the water removal at 0 and 10°C , at -10°C it took place
277 through sublimation which can be assumed to be atmospheric freeze drying. This
278 makes the outer porous dry layer developed during this kind of drying more prone to
279 the ultrasonic effects than the more compact structure developed during drying by
280 evaporation at 0 and 10°C . In this sense, Ozuna, Gómez, Riera, Cárcel, and Garcia-
281 Perez, (2014c) observed that the product porosity influences the extension of the
282 ultrasound effects during drying. Thus, highly porous materials present higher values of
283 impedance, closer to the surrounding air, than materials with a hard and closed-
284 compact structure. The fact that the coupling of the air-porous structure is better makes
285 easier the ultrasound transmission and helps ultrasound effects to be more intense
286 (Ozuna et al., 2014c).

287

288 3.3. Rehydration experiments

289 Since rehydration potential is an important quality attribute for products that need to be
290 reconstituted before consumption, the influence of the drying method on the
291 rehydration kinetics of dried samples (0.54 ± 0.07 kg water/kg dm_{dc}) was experimentally
292 determined. The results obtained showed that the AIR samples dried at -10°C
293 rehydrated significantly ($p<0.05$) faster than those dried at 10 and 0°C (Figure 3).
294 Thereby, the average rehydration time for AIR samples dried at 0 and 10°C was
295 22.0 ± 0.9 h, while for AIR samples dried at -10°C it was 8.7 ± 0.3 h. The moisture content

296 reached at the end of the rehydration process was also significantly ($p < 0.05$) higher for
297 samples dried at -10°C (3.05 ± 0.44 kg water/kg dm_{dc}) than for those dried at 10 and
298 0°C (2.61 ± 0.24 and 2.41 ± 0.10 kg water/kg dm_{dc}, respectively). These results could be
299 explained by the fact that drying at -10°C leads to a minimum shrinkage and a highly
300 porous structure (Stawczyk, Li, Witrowa-Rajchert, and Fabisiak, 2007). So, the high
301 porosity makes it easier for water to enter the dried matrix.

302 The application of US during drying did not significantly ($p < 0.05$) affect the moisture
303 gain rate during the rehydration of samples dried at 0 and 10°C (Figure 3). On the
304 contrary, for samples dried at -10°C , US application slightly reduced the rehydration
305 rate and the final moisture gain. US could affect the microstructure of cod samples,
306 provoking ruptures in the cod fibers and causing the formation of wider spaces
307 between myofibrils (Ozuna et al., 2014c). The extension of these effects were enough
308 to modify the rehydration capacity of cod slices dried at -10°C , but not for those dried at
309 0 and 10°C . It is likely that this is due to the combined impact of freezing and US
310 application on the structure of the samples dried at -10°C , which results in a softer and
311 more unstructured matrix where the water intake and its retention during the
312 rehydration process is more difficult. In this sense, Nowacka, Wiktor, Śledź, Jurek, and
313 Witrowa-Rajchert (2012) reported that a short ultrasonic pretreatment of apple cubes
314 before drying reduced their moisture content after 60 minutes of rehydration due to
315 changes in the product's microstructure. However, Schössler et al. (2012) reported no
316 differences in the rehydration characteristics of the US assisted freeze-dried red bell
317 pepper in comparison with those conventionally freeze-dried, probably due to the lower
318 efficiency of the contact ultrasonic system used in this work.

319 The experimental rehydration kinetics were also modeled, taking Equation 2 into
320 account. A satisfactory description ($\text{VAR} > 98\%$) (Table 2) of the rehydration kinetics
321 was only obtained for AIR dried samples at 0 and 10°C (Figure 3). In samples dried at -

322 10°C, mechanisms other than diffusion, and probably linked to the high porosity and
323 bulk water input, could be involved.

324 The D_{er} identified for samples dried at 0 and 10°C was similar (Table 2). At these
325 temperatures, US application during drying caused a slight but not significant ($p < 0.05$)
326 increase in the D_{er} . However, the D_{er} identified for AIR samples dried at -10°C was five
327 times greater than that identified for those dried at 0 and 10°C. In this case, AIR+US
328 samples dried at -10°C showed a significantly ($p < 0.05$) lower D_{er} than AIR samples.

329

330 3.4. Color

331 3.4.1. Dried samples

332 The average values of the color coordinates of desalted cod before drying were
333 63.7 ± 1.9 for L^* , -3.85 ± 0.52 for a^* and 0.95 ± 0.78 for b^* . In general terms, as can be
334 observed in Table 3, the drying increased the value of the three coordinates. AIR dried
335 samples at 0 and 10°C showed higher a^* and b^* coordinates and lower L^* than those
336 dried at -10°C. These results suggest that the moisture removal by evaporation (0 and
337 10°C) caused a yellowing (higher b^*) and a darkening (lower L^*), while the removal by
338 sublimation (-10°C) leads to brighter and whiter samples. According to Asli and
339 Morkore (2012), cod should preferably have a high lightness value (L^* -value), as the
340 color white is considered positive by consumers. Bjorkevoll, Reboredo, and Fossen
341 (2014) also associated high quality with a whiter and less yellow surface in the sensory
342 evaluation of the heavy salted cod. However, Lauritzsen et al. (2004) reported that the
343 reduction in the water content causes changes in the color of the fish. Brás and Costa
344 (2010) reported an increase in both the lightness (L^*) and yellowness (b^*) of the cod
345 caused by drying, which was more marked as drying progressed.

346 The application of US during drying only significantly ($p < 0.05$) affected the L^*
347 coordinate for samples dried at -10°C, reducing their lightness as compared with AIR

348 samples. Moreover, the overall color difference (ΔE) between samples dried without
349 (AIR) and with (AIR+US) (Table 3) showed negligible differences in the case of
350 samples dried at 0 and 10°C due to the fact that, as reported by Francis and
351 Clydesdale (1975), ΔE values lower than 2 are not detected by the human eye. On the
352 contrary, the ΔE obtained for the samples dried at -10°C was significantly ($p < 0.05$)
353 higher; this indicated that, at this drying temperature, US application caused a
354 meaningful color difference. This was probably due to the slight thermal effect
355 generated by US on the sample's surface, which could be more marked in this case
356 and bring about a little darkening.

357

358 *3.4.2. Rehydrated samples*

359 The drying temperature did not affect the color of the rehydrated samples (Table 4) and
360 no significant ($p < 0.05$) differences were found for samples previously dried at -10, 0 or
361 10°C. In a similar way, US application during drying did not cause noticeable changes
362 in the color coordinates of the rehydrated samples (Table 4).

363 In this case, ΔE was calculated by considering the desalted cod prior to drying as
364 reference. In general terms, the dried and rehydrated cod samples did not recover the
365 color of the desalted samples, the ΔE ranging from 8.8 to 11.7 (Table 4).

366

367 *3.5. Texture*

368 *3.4.1. Dried samples*

369 The initial hardness of the desalted cod was 1.55 ± 0.53 N. Therefore, the drying
370 process provoked a hardening of the samples (Figure 4), regardless of the drying
371 conditions used. For the AIR samples, the hardness was dependent on the drying
372 temperature (Figure 4), so, the lower the air temperature, the harder the dried cod
373 sample. No influence of the air drying temperature on the hardness was observed in

374 the case of AIR+US samples. However, when comparing ultrasonically assisted dried
375 samples with those conventionally dried, it was observed that the AIR+US samples
376 dried at 0 and 10°C were significantly ($p<0.05$) harder than the AIR ones (Figure 4).
377 This fact could be attributed to the successive compression and expansion cycles of
378 the material produced by US, which could affect cod proteins thus causing a hardening
379 of the samples. At -10°C, the hardening of AIR and AIR+US samples was similar. The
380 previous freezing step and the fact that water removal occurred by sublimation could
381 provoke changes in the sample's structure that may mask the structural US effect.

382

383 *3.4.2. Rehydrated samples*

384 In general, both the drying and the later rehydration process produced samples that
385 were slightly harder than the initial desalted cod (1.55 ± 0.53 N), but their final hardness
386 depended on the drying temperature and US application. Thus, in the case of AIR
387 samples, the effect of drying temperature on rehydrated samples was to the opposite of
388 that found in dried samples; so, the higher the air temperature, the harder the
389 rehydrated sample (Figure 5). As regards the application of US, the rehydrated
390 AIR+US samples dried at 0 were significantly ($p<0.05$) harder than AIR samples
391 (Figure 5). The textural changes caused by US application could be linked to the
392 denaturation of proteins (Lee and Feng, 2011). In the case of samples dried at 10°C,
393 no significant ($p<0.05$) differences were observed between AIR and AIR+US, which
394 could be explained by the fact that the shorter drying time at 10°C prevented a lengthy
395 action of US on the internal structure. In the case of -10°C experiments, the effects of
396 freezing on structure can mask the effects of ultrasound.

397

398

399

400 **4. Conclusions**

401 The application of US during the low temperature drying of desalted cod improved the
402 drying rate at every temperature tested, but it was particularly noticeable when drying
403 took place at -10°C, which is when water removal took place by sublimation. As far as
404 quality attributes are concerned, the cod dried at -10°C rehydrated faster and gained
405 more water than that dried at higher temperatures. Moreover, these samples were
406 brighter, whiter and slightly softer than those dried at 0 and 10°C. US application
407 slightly reduced the rehydration rate and increased the sample's hardness, but allowed
408 whiter samples to be obtained, which are usually preferred by consumers. Therefore,
409 power ultrasound could be considered an interesting technology to speed-up the low
410 temperature drying of desalted cod without greatly affecting the quality of the obtained
411 product.

412

413 **Acknowledgements**

414 The authors acknowledge the financial support of the Spanish Ministerio de Economía
415 y Competitividad (MINECO) and the European Regional Development Fund (ERDF)
416 from the project DPI2012-37466-CO3-03 and the FPI fellowship (BES-2010-033460)
417 granted to J.V. Santacatalina. They also wish to acknowledge Carmen Cambra S.L. for
418 their technical support with the selection of the raw material.

419

420 **References**

- 421 Andrés, A., Rodríguez-Barona, S., & Barat, J.M. (2005). Analysis of some cod-
422 desalting process variables. *Journal of Food Engineering*, 70, 67-72.
- 423 Asli, M., & Morkore, T. (2012). Brines added sodium bicarbonate improve liquid
424 retention and sensory attributes of lightly salted Atlantic cod. *LWT-Food*
425 *Science and Technology*, 46, 196-202.

- 426 Association of Official Analytical Chemists (AOAC) (1997). *Official methods of analysis*.
427 Association of Official Analytical Chemists, Arlington, Virginia, USA.
- 428 Bai, J.W., Sun, D.W., Xiao, H.W., Mujumdar, A.S., & Gao, Z.J. (2013). Novel high-
429 humidity hot air impingement blanching (HHAIB) pretreatment enhances drying
430 kinetics and color attributes of seedless grapes. *Innovative Food Science &
431 Emerging Technologies*, 20, 230-237.
- 432 Bantle, M., & Eikevik, T.M. (2011). Parametric study of high intensity ultrasound in the
433 atmospheric freeze drying of peas. *Drying Technology*, 29, 1230-1239.
- 434 Bantle, M., & Hanssler, J. (2013). Ultrasonic convective drying kinetics of clipfish during
435 the initial drying period. *Drying Technology*, 31, 1307-1316.
- 436 Bjorkevoll, I., Reboredo, R.G., & Fossen, I. (2014). Methods for phosphate addition in
437 heavy salted cod (*Gadus morhua* L.). *LWT-Food Science and Technology*, 58,
438 502-510.
- 439 Brás, A., & Costa, R. (2010). Influence of brine salting prior to pickle salting in the
440 manufacturing of various salted-dried fish species. *Journal of Food Engineering*,
441 100, 490-495.
- 442 Cárcel, J.A., Garcia-Perez, J.V., Riera, E., & Mulet, A. (2011). Improvement of
443 convective drying of carrot by applying power ultrasound-Influence of mass load
444 density. *Drying Technology*, 29, 174-182.
- 445 Claussen, I.C., Ustad, T.S., Strømmen, I., & Walde, P.M. (2007). Atmospheric freeze
446 drying - A review. *Drying Technology*, 25, 957-967.
- 447 Crank, J. (1975). *The Mathematics of Diffusion*. Oxford University Press, London, UK.
- 448 Fernández-Segovia, I., Escriche, I., Fuentes, A., & Serra, J.A. (2007). Microbial and
449 sensory changes during refrigerated storage of desalted cod (*Gadus morhua*)
450 preserved by combined methods. *International Journal of Food Microbiology*,
451 116, 64-72.

- 452 Francis, F.J., & Clydesdale, F.M. (1975). *Food colorimetry: Theory and applications*.
453 AVI Publishing Co. Inc., New York, USA.
- 454 Gallego-Juárez, J.A., Riera, E., de la Fuente Blanco, S., Rodríguez-Corral, G., Acosta-
455 Aparicio, V.M., & Blanco, A. (2007). Application of high-power ultrasound for
456 dehydration of vegetables: processes and devices. *Drying Technology*, 25,
457 1893-1901.
- 458 Gallego-Juárez, J.A. (2010). High-power ultrasonic processing: Recent developments
459 and prospective advances. *Physics Procedia*, 3, 35-47.
- 460 Garau, M.C., Simal, S., Femenia, A., & Rosselló, C. (2006). Drying of orange skin:
461 drying kinetics modelling and functional properties. *Journal of Food*
462 *Engineering*, 75, 288-295.
- 463 Garcia-Perez, J.V., Ozuna, C., Ortuño, C., Cárcel, J.A., & Mulet, A. (2011). Modeling
464 ultrasonically assisted convective drying of eggplant. *Drying Technology*, 29,
465 1499-1509.
- 466 Garcia-Perez, J.V., Cárcel, J.A., Riera, E., Rosselló, C., & Mulet, A. (2012).
467 Intensification of low temperature drying by using ultrasound. *Drying*
468 *Technology*, 30, 1199-1208.
- 469 Lauritzsen, K., Akse, L., Johansen, A., Joensen, S., Sørensen, N.K., & Olsen, R.L.
470 (2004). Physical and quality attributes of salted cod (*Gadus morhua* L.) as
471 affected by the state of rigor and freezing prior to salting. *Food Research*
472 *International*, 37, 677-688.
- 473 Lee, H., & Feng, H. (2011). Effect of Power Ultrasound on Food Quality. In: *Ultrasound*
474 *Technologies for Food and Bioprocessing*, Feng, H., Barbosa-Cánovas, G.V., &
475 Weiss, J., Eds., Springer, New York, 559-582.

- 476 Martínez-Álvarez, O., & Gómez-Guillén, C. (2013). Influence of mono- and divalent
477 salts on water loss and properties of dry salted cod fillets. *LWT-Food Science
478 and Technology*, 53, 387-394.
- 479 Nowacka, M., Wiktor, A., Śledź, M., Jurek, N., & Witrowa-Rajchert, D. (2012). Drying of
480 ultrasound pretreated apple and its selected physical properties. *Journal of
481 Food Engineering*, 113, 427-433.
- 482 Oliveira, H., Pedro, S., Nunes, M.L., Costa, R., & Vaz-Pires, P. (2012). Processing of
483 salted cod (*Gadus* spp.): A review. *Comprehensive Reviews in Food Science
484 and Food Safety*, 11, 546-564.
- 485 Ozuna, C., Puig, A., Garcia-Perez, J.V. & Cárcel, J.A. (2014a). Ultrasonically enhanced
486 desalting of cod (*Gadus morhua*). Mass transport kinetics and structural
487 changes. *LWT-Food Science and Technology*, 59, 130-137.
- 488 Ozuna, C., Cárcel, J.A., Walde, P.M. & Garcia-Perez, J.V. (2014b). Low-temperature
489 drying of salted cod (*Gadus morhua*) assisted by high power ultrasound:
490 Kinetics and physical properties. *Innovative Food Science and Emerging
491 Technologies*, 23, 146-155.
- 492 Ozuna, C., Gómez, T., Riera, E., Cárcel, J.A., & Garcia-Perez, J.V. (2014c). Influence
493 of material structure on air-borne ultrasonic application in drying. *Ultrasonics
494 Sonochemistry*, 21, 1235-1243.
- 495 Pingret, D., Fabiano-Tixier, A.S., & Chemat, F. (2013). Degradation during application
496 of ultrasound in food processing: A review. *Food Control*, 31, 593-606.
- 497 Santacatalina, J.V., Rodríguez, O., Simal, S., Cárcel, J.A., Mulet, A., Garcia-Perez, J.V.
498 (2014). Ultrasonically enhanced low-temperature drying of apple: Influence on
499 drying kinetics and antioxidant potential. *Journal of Food Engineering*, 138, 35-
500 44.

- 501 Schössler, K., Jäger, H., & Knorr, D. (2012). Novel contact ultrasound system for the
502 accelerated freeze-drying of vegetables. *Innovative Food Science and*
503 *Emerging Technologies*, 16, 113-120.
- 504 Soria, A.C., Corzo-Martínez, M., Montilla, A., Riera, E., Gamboa-Santos, J., & Villamiel,
505 M. (2010). Chemical and physicochemical quality parameters in carrots
506 dehydrated by power ultrasound. *Journal of Agricultural and Food Chemistry*,
507 58, 7715-7722.
- 508 Stawczyk, J., Li, S., Witrowa-Rajchert, D., & Fabisiak, A. (2007). Kinetics of
509 atmospheric freeze-drying of apple. *Transport in porous media*, 66, 159-172.
- 510

511

Figure captions

512

513 **Figure 1.** Diagram of the ultrasonically assisted convective dryer: 1, fan; 2, Pt-100; 3,
514 temperature and relative humidity sensor; 4, anemometer; 5, ultrasonic transducer; 6,
515 vibrating cylinder; 7, sample load device; 8, retreating pipe; 9, slide actuator; 10,
516 weighing module; 11, heat exchanger; 12, heating elements; 13, desiccant tray
517 chamber; 14, details of the sample load on the trays.

518

519

520 **Figure 2.** Experimental and calculated (diffusion model) drying kinetics (2 m/s) of
521 desalted cod at different temperatures (-10, 0 and 10°C), without (AIR) and with
522 (AIR+US, 20.5 kW/m³, 21 kHz) ultrasound application.

523

524 **Figure 3.** Experimental and calculated (diffusion model) rehydration kinetics of
525 desalted and dried cod (2 m/s) at different temperatures (-10, 0 and 10°C), without
526 (AIR) and with (AIR+US, 20.5 kW/m³, 21 kHz) ultrasound application.

527

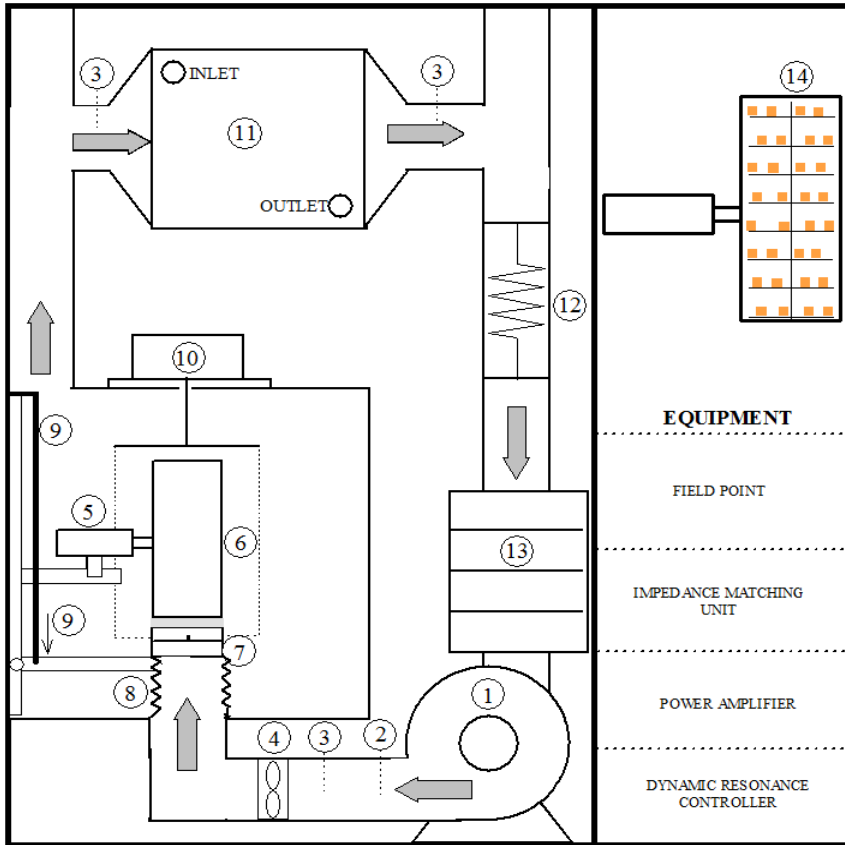
528 **Figure 4.** Hardness of desalted and dried cod at different temperatures (-10, 0 and
529 10°C), without (AIR) and with (AIR+US, 20.5 kW/m³, 21 kHz) ultrasound application.
530 Average values ± LSD intervals (p<0.05) are plotted. Different letters show significant
531 differences according to LSD intervals (p<0.05).

532

533 **Figure 5.** Hardness of rehydrated cod previously desalted and dried at different
534 temperatures (-10, 0 and 10°C), without (AIR) and with (AIR+US, 20.5 kW/m³, 21 kHz)
535 ultrasound application. Average values ± LSD intervals (p<0.05) are plotted. Different
536 letters show significant differences according to LSD intervals (p<0.05).

537

538



539

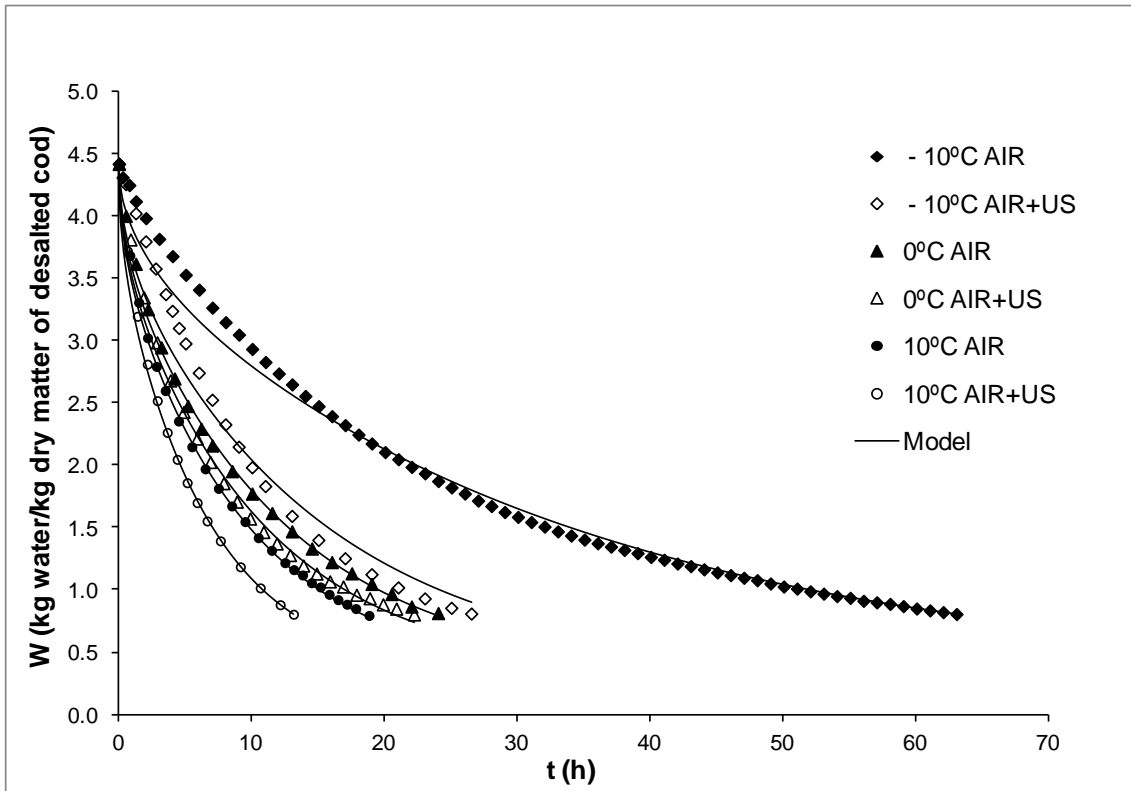
540

541

542

Figure 1

543



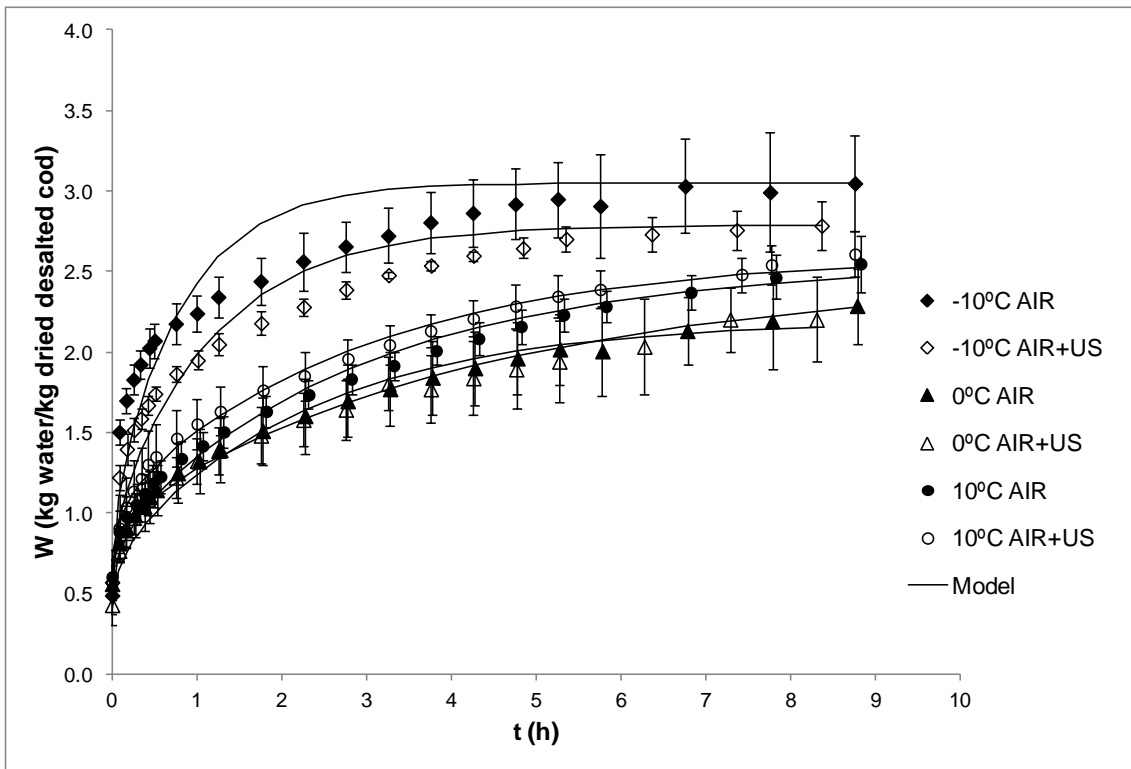
544

545

546

547

Figure 2



549

550

551

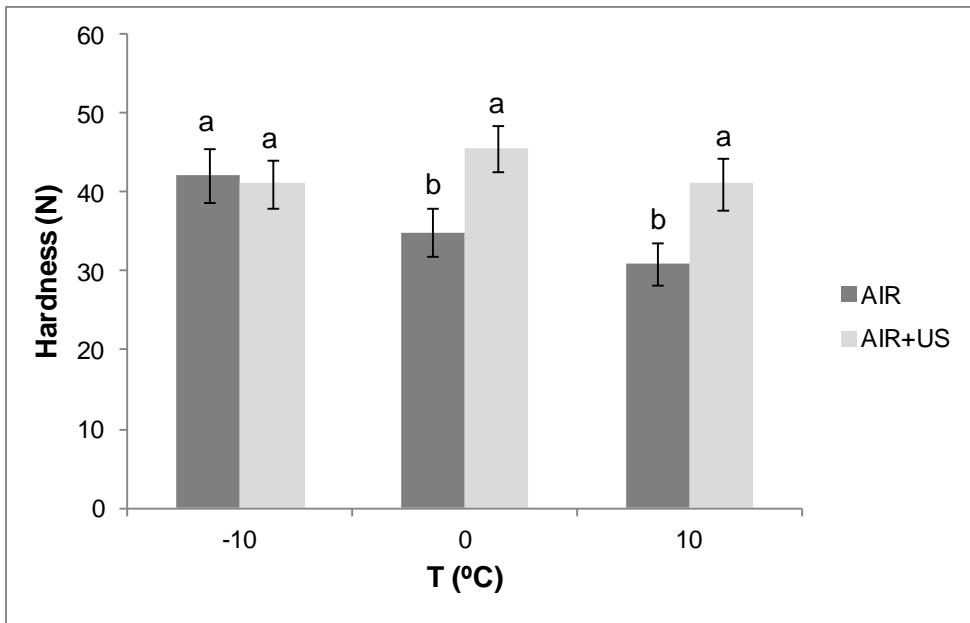
Figure 3

552

553

554

555



556

557

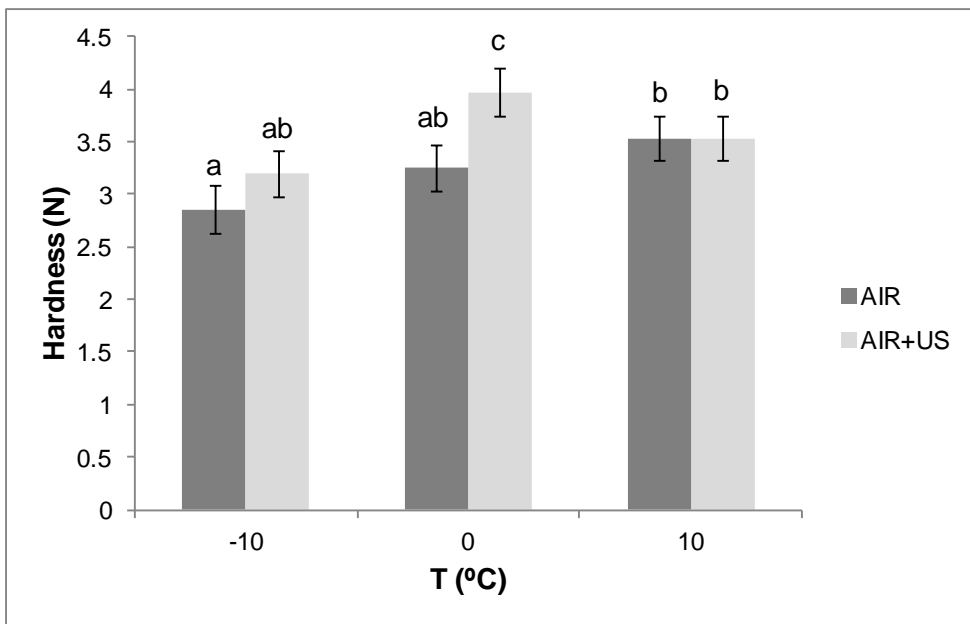
558

Figure 4

559

560

561



562

563

564

Figure 5

565

566

567

568 Table 1. Effective moisture diffusivity (D_{ed}) for the drying kinetics of desalted cod at
569 different temperatures (10, 0 and -10°C), without (AIR) and with (AIR+US, 20.5 kW/m^3 ,
570 21 kHz) ultrasound application. Average values \pm standard deviation are shown. VAR
571 (%) is the percentage of explained variance. ΔD_{ed} shows (in percentage) the increase
572 in effective moisture diffusivity produced by ultrasonic application.

T ($^{\circ}\text{C}$)	AIR		AIR+US		ΔD_{ed} (%)
	D_{ed} ($10^{-11}\text{ m}^2/\text{s}$)	VAR (%)	D_{ed} ($10^{-11}\text{ m}^2/\text{s}$)	VAR (%)	
10	7.77 ± 0.62^e	99.7	10.51 ± 0.33^f	99.1	35.4
0	5.65 ± 0.35^c	99.3	6.63 ± 0.09^d	99.2	17.4
-10	2.17 ± 0.20^a	98.5	4.84 ± 0.60^b	94.4	123.5

573

574

575

576

577

Superscript letters (a, b, c, d, e, f) show homogeneous groups established from LSD (Least Significance Difference) intervals ($p < 0.05$).

578

579 Table 2. Effective moisture diffusivity (D_{er}) for the rehydration kinetics of desalted cod
580 dried at different temperatures (10, 0 and -10°C), without (AIR) and with (AIR+US, 20.5
581 kW/m^3 , 21 kHz) ultrasound application. Average values \pm standard deviation are
582 shown. VAR (%) is the percentage of explained variance.

T ($^{\circ}\text{C}$)	AIR		AIR+US	
	D_{er} ($10^{-10} \text{ m}^2/\text{s}$)	VAR (%)	D_{er} ($10^{-10} \text{ m}^2/\text{s}$)	VAR (%)
10	$1.99 \pm 0.66^{a,b}$	99.1	$2.26 \pm 0.87^{a,b}$	97.5
0	1.89 ± 0.52^a	98.3	$2.34 \pm 0.58^{a,b}$	95.5
-10	9.93 ± 4.35^c	86.7	5.60 ± 2.17^b	94.3

583

584

585

586

Superscript letters (a, b, c) show homogeneous groups established from LSD (Least Significance Difference) intervals ($p < 0.05$).

587
 588 Table 3. CIELab (L*, a*, b*) color coordinates for desalted cod dried at different
 589 temperatures (10, 0 and -10°C), without (AIR) and with (AIR+US, 20.5 kW/m³,
 590 21 kHz) ultrasound application. Average values ± standard deviation are shown.
 591 ΔE represents the overall color differences between AIR+US and AIR samples.

		-10°C	0°C	10°C
L*	AIR	79.9±4.4 ^a	57.9±4.1 ^c	54.1±2.3 ^{c,d}
	AIR+US	67.0±4.3 ^b	55.3±4.2 ^{c,d}	55.9±5.0 ^d
a*	AIR	-1.2±0.4 ^m	-1.0±1.3 ^m	-0.1±1.2 ⁿ
	AIR+US	-0.9±0.5 ^m	-1.0±0.8 ^m	-1.0±1.0 ^m
b*	AIR	13.6±3.0 ^x	16.1±3.0 ^y	16.1±2.9 ^y
	AIR+US	12.6±2.6 ^x	15.8±2.6 ^y	15.6±3.0 ^y
ΔE	AIR+US vs AIR	12.9	2.6	2.1

592 Superscript letters (a, b, c, d), (m, n) and (x, y) show homogeneous groups, established from LSD (Least Significance
 593 Difference) intervals (p<0.05) for L*, a* and b*, respectively.
 594
 595

597

598

599